

Study on the influence of the abrasion angle on the rubber abrasion performance at different scales

Z. Wang*, Sh. Hu, F. Zhang, L. Ma*

School of Electromechanical Engineering, Qingdao University of Science and Technology, Qingdao, Shandong, China

Received September 28, 2017; Accepted December 19, 2017

Rubber abrasion experiments under different temperatures and angles were carried out using a high temperature rubber abrasion tester to study the influence of temperatures and angles on the rubber abrasion performance. Surface morphology images of rubber samples were obtained using a 3D measuring laser microscope and their corresponding surface characteristic parameters were then obtained including the arithmetic mean deviation of outline (Ra), the root mean square deviation of outline (Rq), the 3D arithmetic mean deviation (Sa) and the 3D root mean square deviation (Sq). The scale effect on roughness measurements of the rubber abrasion surface was also investigated and an optimal magnification multiple in the microscope was recommended based on the variation data of the line roughness and the surface roughness at various magnifications.

Key words: Rubber composites, Rubber abrasion, Surface morphology, Scale effect

AIMS AND BACKGROUND

As an important industrial raw material, rubber has many advantageous performance characteristics. Improving abrasion performance of rubber products can not only bring considerable economic and social benefits but also enhance products' safety and working life.

In abrasion tests, a series of abrasion patterns on the rubber surface, called Schallamach abrasion patterns [1,2], would be produced with parallel ridges perpendicular to the sliding direction. After numerous experiments, an abrasion model based on the failure mechanism was proposed by some researchers [3-9]. Most of the previous abrasion experiments were carried out at room temperature. Many surface characteristics in the abrasion process and the temperature effect on the abrasion performance were rarely investigated, and it is necessary to identify and investigate the scale range and the optimal scale in the study of the self-affinity fractal characteristics and to determine the upper and lower boundaries of the scale range of self-affinity fractal [10-12].

In this paper, a high-temperature abrasion test was conducted to measure the rubber abrasion volume under different angles and the corresponding surface morphology and microstructure characteristic parameters were obtained using a 3D measuring laser microscope. The relationship between the rubber abrasion performance and the surface morphology characteristics was identified and analyzed.

EXPERIMENTAL

Experimental materials and instruments

Tread rubber from an all-steel radial tire was investigated. The equipment used in the experiment included a rubber mixer (XSM-500), a roll mill (BL-6175-BL), a plate vulcanizing apparatus (HS-100T-FTMO-2PT), a rotorless curemeter (GT-M2000-A), a densimeter (GT-XS-365M), a double- end grinding machine (MZ-4101), a 3D measuring laser microscope (LEXT OLS4100) and a new type of abrasion tester intentionally designed for more realistic abrasion studies.

Experimental procedures

Step 1. Prepare rubber samples and paste them to a heatable wheel. Then place the wheel in a vulkometer and bake at 115°C for 2.5 h. After that, cool the wheel at room temperature for 24 h.

Step 2. Install the cooled rubber wheel on a rubber abrasion tester and heat it by a heating system to a desired temperature based on the experimental matrix.

Step 3. Start and operate the rubber abrasion tester for 500 revolutions as a pre-grinding. Then, weigh the rubber wheel and rubber strips after taking it off from the tester and cleaning it up and mark the total mass as m_1 .

Step 4. Install the rubber wheel on the tester again and operate the tester for 1709 revolutions (500 meters). Then, the total mass of the wheel and rubber strips m_2 is obtained, after taking off and cleaning up.

Step 5. Calculate the abrasion volume using the following equation according to GB/T533:

$$V=(m_1-m_2)/\rho \quad (1)$$

To whom all correspondence should be sent:
E-mail: wzp_ww1@163.com

V - abrasion volume of the sample, cm^3 .

m_1 - mass of the sample after pre-grinding, g.

m_2 - mass of the sample after test, g.

ρ - density of the sample, g/cm^3 .

RESULTS AND DISCUSSION

Abrasion tests under different angles and temperatures were carried out under a load of 26.70N on the high temperature rubber abrasion tester with a 40# abrasion wheel. The tests were replicated several times for a given angle and temperature and the average values were adopted as the experimental data. Table 1 shows the experimental results at various combinations of temperatures and angles. It is seen from the table that the abrasion volume increases as the angle and temperature increase. Namely, the abrasion volume is the greatest at 21° angle and the smallest at 9° angle and in between for other angles. Similarly, the abrasion volume is the greatest at 80 °C and the smallest at 25 °C and in between at 60 °C.

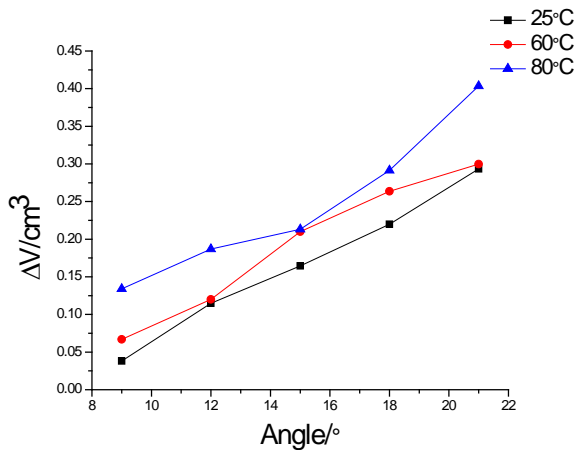


Fig. 1. Relation between the abrasion volume and the angle

Table 1. Experimental results for the abrasion of rubber strips

Temperature / °C	Angle / °	ρ / (g/cm^3)	m_1 / g	m_2 / g	Δm / g	ΔV / cm^3
25	9	1.131	69.975	69.932	0.043	0.0380
25	12	1.106	69.002	68.875	0.127	0.1148
25	15	1.101	65.616	65.435	0.181	0.1644
25	18	1.105	67.241	66.998	0.243	0.2199
25	21	1.101	68.325	68.002	0.323	0.2934
60	9	1.105	67.757	67.683	0.074	0.0670
60	12	1.074	66.821	66.692	0.129	0.1201
60	15	1.105	65.446	65.214	0.232	0.2100
60	18	1.096	68.023	67.734	0.289	0.2637
60	21	1.104	76.262	75.931	0.331	0.2998
80	9	1.096	68.177	68.030	0.147	0.1341
80	12	1.081	76.429	76.227	0.202	0.1869
80	15	1.104	67.329	67.094	0.235	0.2131
80	18	1.115	67.612	67.287	0.325	0.2915
80	21	1.105	67.556	67.110	0.446	0.4036

Analysis of the abrasion value

According to the experimental results in Table 1, the relation between the abrasion volume and the angle is plotted in Fig. 1. It is also observed from the above experimental results that the abrasion volume increases with the increase in temperature. Due to its viscoelasticity and large deformation under cyclic loading, rubber usually shows a strong time lag behavior in the dynamic changing process accompanied with a large quantity of heat generation, which leads to a sharp temperature rise in the rubber sample over time. Under heating, the physicochemical properties of rubber are significantly different from those at room temperature. At high temperature, the molecular thermal motion energy in rubber composites increases and its kinematic component becomes more active, which leads to thermal decomposition of the rubber material and results in changes in the rubber surface microstructure, the molecular chain form, the chain conformation and mesh structure inside the rubber, the degree of pyrolysis of the materials and the surface structure. Meanwhile, the viscosity within rubber would drop, which further affects material properties like strength, elasticity modulus and dynamic behavior, and deteriorates the abrasion resistance. Furthermore, the abrasion performance becomes unstable at high temperature. That is why the relation between the abrasion volume and the angle shows great fluctuations.

Abrasion surface analysis

Both 2D and 3D images of rubber abrasion surface morphologies at different angles were obtained at 25 °C using load of 26.70N for the 40# abrasion wheel, as shown in Fig. 2.

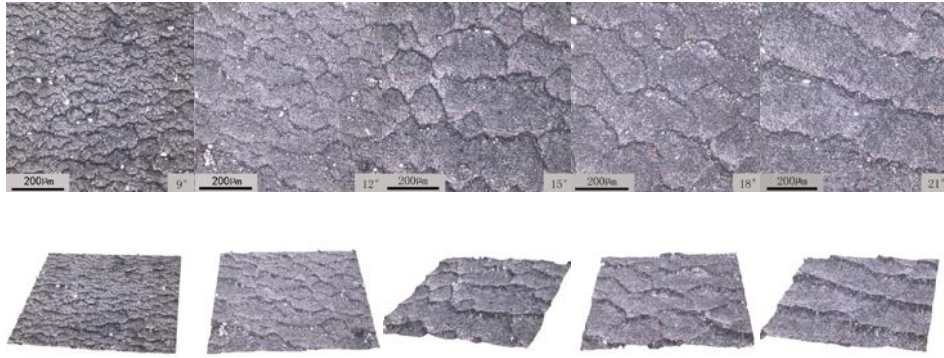


Fig. 2. 2D and 3D microscope images of abrasion surface under different angles

It can be seen from Fig. 2 that the abrasion surface evolves from a tiny scaly abrasion pattern to a strip mill grain as the angle increases and the grinding grain spacing and depth gradually increase. It is indicated that the friction stress between the rubber surface and the grinding wheel is lower under a smaller angle and thus the shear force in the rubber chain is also lower at small angles, which increases its ability to tear. As the angle continuously increases, the friction stress between the rubber surface and the grinding wheel gradually increases and the shear stress in the rubber molecular chain also increases, which deteriorate the rubber’s ability to resist tear. At larger angles, abrasion is severe as the grains continue to grow and the tear formation pit contour continues to expand. In the meantime, the flaky grinding pattern becomes a ladder-shape grinding pattern and the surface becomes rougher. Therefore, the greater the angle, the higher is the friction stress and the more severe is the abrasion. As the grinding pattern spacing and height increase, the abrasion surface becomes more complicated too.

To further explore the characteristics of the abrasion surface morphology, its variation with the angle can be described with R_a , R_q , S_a and S_q , where R_a represents the arithmetic mean of the distance between the points on the outline and the datum line in the sampling length; R_q represents the root mean square height of the outline in the sampling length; S_a is an index to characterize the surface roughness in the microscopic field scale and S_q is the standard deviation of the surface height distribution.

Those characteristic parameters describing the rubber abrasion surfaces, as shown in equations (1) to (4), were obtained for angles 9°, 12°, 15°, 18° and 21° using the 3D measuring laser microscope under load of 26.70N and temperature of 25 °C for the 40# abrasion wheel, as shown in Table 2.

The experimental data in Table 2 can also be illustrated in the line chart shown in Fig. 3.

Table 2. Characteristic parameters of the surface under different angles

Angle / °	$R_a / \mu\text{m}$	$R_q / \mu\text{m}$	$S_a / \mu\text{m}$	$S_q / \mu\text{m}$
9	0.915	1.150	1.124	1.537
12	0.935	1.177	1.145	1.528
15	1.110	1.435	1.347	1.894
18	1.348	1.772	1.611	2.316
21	1.476	1.934	1.684	2.589

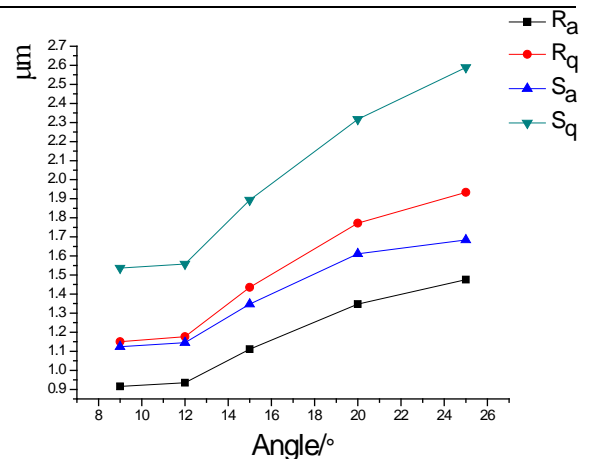


Fig. 3. Line chart of R_a , R_q , S_a and S_q and angle

It is seen from Fig. 3 that the characteristic parameters R_a , R_q , S_a and S_q continuously increase with angle increase. Their increase is almost neglectable for angles less than 12°. As defined, R_a and R_q are related to the height of contour convex peaks, their greater values at higher angles indicate that the abrasion marks have gradually changed from an abrupt morphology to a gentle one. In addition, the height of contour convex peaks increases with more fluctuation and the abrasion surface becomes rougher. S_a and S_q can be used to describe the abrasion surface height and its distribution, respectively. The higher values of S_a and S_q at greater angles shown in Table 2 and Fig. 3 indicate a more dispersive surface height and a more severe and complex abrasion surface

morphology. These results are consistent with the results depicted in Fig. 2.

Scale effect in roughness measurements

The contours of the curve images from the abrasion surface morphology of the rubber sample tested under the condition of 15° angle, 80 °C temperature, 26.70N load and 40# wheel were collected by a 3D measuring laser microscope using different observation scales. The microstructure of the abrasion surface outline shows some self-similarities and the abrasion surfaces display similar microscopic features as hierarchy nesting of infinite levels under different observation scales. The line roughness parameters on rubber abrasion surfaces at different observation scales were obtained under the test conditions of 15° angle, 80 °C temperature, 26.70N load and 40# wheel using the 3D measuring laser microscope, as shown in Table 3.

Table 3. Line roughness parameters under different observation scales

Magnification multiples	R _a / μm	R _q / μm	R _{sk}
108	1.111	1.343	0.057
216	1.168	1.467	0.098
324	1.292	1.636	0.195
427	1.315	1.649	0.208
555	1.375	1.726	0.239
640	1.296	1.590	0.173
769	0.319	0.396	0.075
854	0.144	0.175	0.031

The experimental data in Table 3 are also replotted in Fig. 4.

Characteristic parameters *R_a*, *R_q* and *R_{sk}* initially increase with an increased magnification multiples, then start to decrease after magnification multiples greater than 550 and finally rapidly drop when the magnification multiple reaches 769. This suggests that a finer surface profile structure would

be collected at miniature observation scales, which results in slightly increased line roughness parameters. However, the further identification and characterization of the microstructural level is limited by the resolution of the measuring instrument (resolution limits) and the rubber surface structure itself (physical limits).

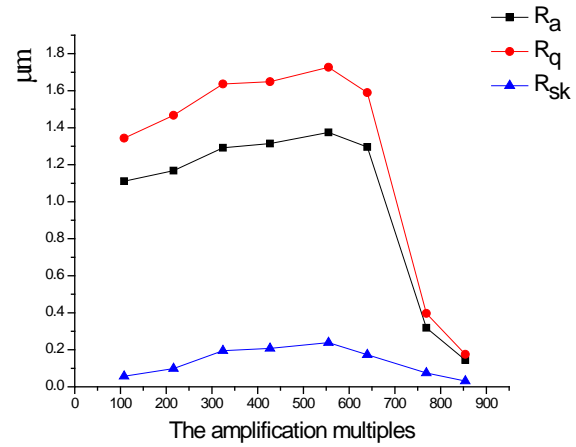


Fig. 4. Values of *R_a*, *R_q* and *R_{sk}* at different amplification multiples

When the magnification multiple is greater than 769, only two or three abrasion patterns can be observed within observation area and thus the associated surface characteristic parameters would not reflect the true structural characteristics of the rough surface. Therefore, the magnification should be controlled at 324-640 during the measurement of the characteristic parameters of the surface roughness.

The 2D images of the abrasion surface morphologies at different observation scales were also collected using the 3D measuring laser microscope for the rubber sample tested under the conditions of 15° angle, 80 °C temperature and 26.70N load and 40# wheel. The images are shown in Fig. 5.

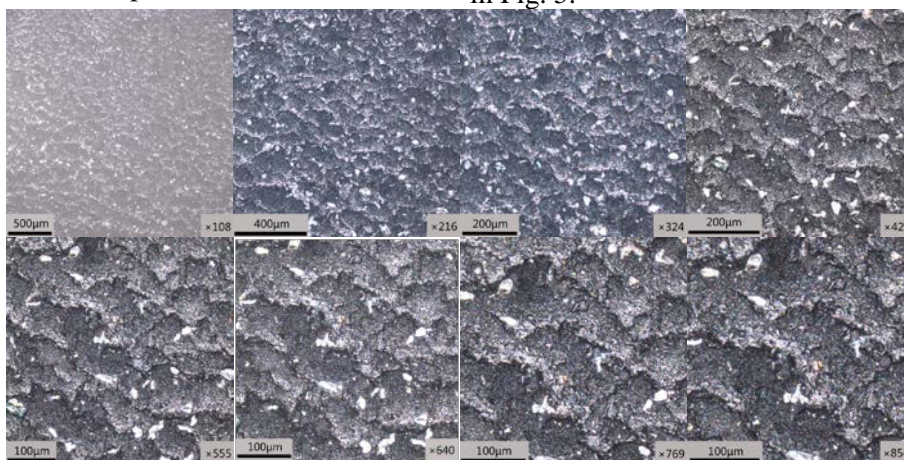


Fig. 5. 2D images of abrasion surface under different magnifications

The corresponding surface roughness parameters of rubber abrasion surfaces at different observation scales are given in Table 4.

Table 4. Surface roughness parameters under different observation scales

Magnification multiples	$S_a / \mu\text{m}$	$S_q / \mu\text{m}$	S_{ku}
108	1.782	2.403	6.792
216	1.767	2.385	6.566
324	1.708	2.311	6.564
427	1.680	2.298	6.358
555	1.658	2.238	6.272
640	1.629	2.189	5.911
769	1.606	2.146	5.662
854	1.583	2.101	5.157

The experimental data in Table 4 can be displayed in graphical form, as shown in Fig. 6.

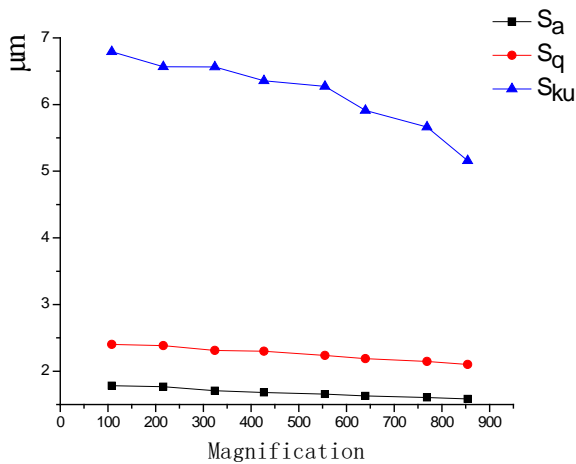


Fig. 6. Variation image of S_a , S_q and S_{ku} with magnification

It is seen from Fig. 6 that the characteristic parameters S_a , S_q and S_{ku} gradually decrease as magnification multiples increase, as expected since the surface roughness parameters were calculated based on the entire image range at a given magnification multiple. The abrasion surface would be reduced in the viewable region of the microscope with a small observation scale and thus the observed abrasion patterns would be enlarged and refined. In addition, the observation area would contain less information on the changes in the abrasion pattern and the corresponding measurements may miss some of the asperity structures that contribute to the rough surface, which would result in a reduced value of surface roughness.

Based on the above results and data analysis of the line roughness and surface roughness from rubber abrasion surface morphology, it is recommended that the best observation magnification is within 324-640.

CONCLUSIONS

The rubber abrasion performance and surface morphology characteristics at various angles were investigated from the perspectives of the abrasion volume and the characteristic parameters of abrasion surfaces under different scales. Based on the above studies, some conclusions can be made:

(1) The angle has a significant influence on the rubber abrasion performance. The abrasion volume increased proportionally with the increase in angle. At higher temperatures, the dependence of the rubber abrasion performance on the angle becomes more uncertain and shows a great fluctuation in data.

(2) The characteristic parameters of the abrasion surface increase with the increase in angle. The larger angle could lead to more severe abrasion and result in a more complex abrasion surface morphology.

(3) The microstructure of the abrasion surface morphology shows a self-similarity structure and its roughness measurement depends upon the scales used in the measurement. The magnification multiple should be kept within 324-640 in the study of rubber abrasion surface morphology.

Acknowledgements: This research was funded by the National Natural Science Foundation of China (51576102), the Science and Technology Program of Shandong Higher Education (J16LB09), the Green Tire and Rubber Collaborative Innovation Project (2015GTR0018).

REFERENCES

1. J. Chen, J. A. Donovan, *Xiangjiao Cankaoziliao*, **25**(7), 50 (1995).
2. P. Thavamani, A. K. Bhowmick, *J. Mater. Sci.*, **28**(5), 1351(1993).
3. B. Lorenz, B.N.J. Persson, S. Dieluweit, T. Tada, *J. Eur. Phys. E*, **34**, 129 (2011).
4. A. Shojaei, M. Arjmand, A. Saffar, *J. Mater. Sci.*, **46**, 1890 (2011).
5. M. Arjmand, A. Shojaei, *Tribol. Lett.*, **41**, 325 (2011).
6. B.N.J. Persson, *Phys. Rev. Lett.*, **87**(11), 116101 (2001).
7. B.N.J. Persson, *Phys. Rev. Lett.*, **89**(24), 245502 (2002).
8. B.N.J. Persson, F. Bucher, B. Chiaia, *Phys. Rev. B*, **65**(18), 184106 (2002).
9. Z. Li, Experimental Study and Numerical Analysis of Tire Tread Wear Behavior. Hefei: University of Science and Technology of China, 2013.
10. J. N. Wang, H. P. Xie, X. Y. Tian, K. Marek, *Chinese J. Rock Mech. & Eng.*, **19**(1), 11(2000).
11. H. P. Xie, Introduction to Fractal-rock Mechanics. Beijing: Science Press, 1997.
12. P. Cao, L. Luo, T. Y. Liu, K. Zhang, *Sci. Tech. Rev.*, **29**(24), 57 (2011).